Theor Appl Climatol (2017) 128:905–917
DOI 10.1007/s00704-016-1746-5

ORIGINAL PAPER

Influences of elevated heating effect by the Himalaya on the changes in Asian summer monsoon

Bian He[1,2]

Received: 8 August 2015 / Accepted: 24 January 2016 / Published online: 10 February 2016

Abstract Based on a series of topographical and thermal sensitivity experiments, the physical processes on the changes of Asian summer monsoon caused by the Himalaya elevated heating were investigated. Six different Himalaya–Iranian Plateau mountain heights were used: 0, 20, 40, 60, 80, and 100 % in the first group (called HIM). The no sensible heating experiments (called HIM_NS) were also performed with the same six mountain heights, but the surface sensible heating was not allowed to heat the atmosphere. The results indicate that the elevated heating effect of the Himalaya gradually intensified when the Himalaya uplifts. The establishment of SASM over the South Asian land which is characterized by the strong precipitation over south slope of the Tibetan Plateau and the huge warm anticyclone in the upper troposphere are in proportion to the elevated heating effect of the Himalaya. Further analysis suggests that the surface heat fluxes over the Himalaya keep almost unchanged during the uplifting, but the lifted condensation level reduces gradually over the regions where the mountain uplifts. The condensation moisturing increases correspondingly and leads to the increase of latent heating in the upper troposphere. Therefore, the positive feedback between the moist convection over the south slope of the Himalaya and monsoon circulation over Indian subcontinent forms and the successive precipitation over the South Asian land is maintained.

✉ Bian He
heb@lasg.iap.ac.cn

[1] State Key Laboratory of Numerical Modeling for Atmospheric Sciences and Geophysical Fluid Dynamics, Institute of Atmospheric Physics, Chinese Academy of Sciences, Beijing 100029, China

[2] State Key Laboratory of Loess and Quaternary Geology, Institute of Earth Environment, Chinese Academy of Sciences, Xi'an 710075, China

1 Introduction

The highlands in the world are important topographical forcings to the global climate change. The Tibetan Plateau (TP) located in the Asian continent is the largest mountain where on its south edge there lies the Himalaya, the highest peak in the world. Previous studies documented that the existence of Tibetan Plateau (TP) has close relationships with the formation and variation of the Asian summer monsoon (Manabe and Terpstra 1974; Wu and Zhang 1998; Duan and Wu 2005; Zhang et al. 2006; Kitoh et al. 2010; Liu et al. 2012). Hahn and Manabe (1975) tested mountain to no-mountain experiments in a general circulation model (GCM) and found the South Asian summer monsoon (SASM) cannot extend north to the Asian inland if the topography of TP is removed in the model. More complex experiments such as testing different topographic heights of the TP in the GCMs have been performed in later studies (Chen et al. 1999; Liu 1999; Kitoh 2004; Jiang et al. 2008), their results show an identical conclusion that the with the uplift of the TP height from 0 to the contemporary era height, the South Asian summer monsoon precipitation extends gradually from the Indian Ocean to the Asian inland with the peak monsoon precipitation occurring on the south slope of the Himalaya which is similar to the evolution of the observed Asian summer monsoon precipitation. Moreover, Liu and Yin (2002) indicated that the evolution of East Asian monsoon is more sensitive to the uplift of the Tibetan Plateau than that of the South Asia monsoon. Kitoh (2004) suggested that the increasing of precipitation over Asia reaches a threshold when the TP is uplifted to 60 % of its realistic altitude.

Recently, more and more studies revealed that the response of Asian summer monsoon is quite sensitive to thermodynamic forcing in different subregions of TP. Boos and Kuang (2010) showed the spatial pattern and strength of the SASM are almost unaffected when the plateau part of TP is removed but the Himalaya is preserved. Similar results had been achieved by Tang et al. (2013) with regional model. They suggested that the Indian summer monsoon is primarily intensified by the forcing of southern TP while the East Asian summer monsoon is mainly enhanced by the forcing of the central TP. Zhang et al. (2012) who used CAM4 to test the different subregional uplifts within the Himalaya–Tibetan Plateau on Asian summer monsoon evolution and found that the increasing precipitation over South Asia is more sensitive to Himalaya uplift. In a word, a number of recent numerical experiments show that the existence of the Himalaya is more important than the whole TP in controlling evolutions of SASM.

However, the associated physical process that the Himalaya modulating the Asian summer monsoon is still not clear. Boos and Kuang (2010, 2013) emphasized the blocking effect of the Himalaya produce strong SASM by insulating warm, moist air over continental India from the cold and dry extratropics while its thermal forcing is not important. Nevertheless, Wu et al. (2012a) indicated that the experiment in Boos and Kuang (2010) still contains the heating effect of the Himalaya mainly on its south slope which could act as a strong heating source to produce monsoon precipitation and circulation. Analogously, in the series studies of the topography uplift experiments (Chen et al. 1999; Liu 1999; Kitoh 2004; Jiang et al. 2008), the extension of Asian summer monsoon is the results of the combined effects of thermal and mechanical forcing by the uplifted TP, and the physical processes related to the Asian summer monsoon evolution are not clearly demonstrated. It is necessary to take additional thermal experiments on the uplifted Himalaya to further address the role of the Himalaya in producing strong Asian summer monsoon and the associated physical processes.

Therefore, this article attempts to clarify several specific scientific questions in studying the role of the Himalaya in Asian monsoon dynamics: whether is the elevated heating effect of the Himalaya important than the non-elevated heating in producing strong Asian summer monsoon over Asian continent? If elevated heating is crucial, what is the decisive factor of the heating effect, the increased elevation, or its thermal properties? And what is the associated physical process? To address these issues, we here carry out a series orographical and thermal experiments based on progressive idealized Himalaya–Iranian Plateau uplift and investigate the differences between heating and no heating experiments. The remainder parts of the paper are arranged as follows: Section 2 introduces the model we used and the experimental design. Section 3 presents the simulation results: the responses in monsoon precipitation and circulation to elevated heating of the Himalaya. Section 4 analyzes the changes in diabatic heating and moist process to reveal the processes of the Himalaya elevated heating effect in modulating monsoon activities. Section 5 shows the final conclusions and discussions.

2 Model, datasets, and experimental design

2.1 Model and datasets

The general circulation model used here is the version-2 Spectral Atmosphere Model developed at IAP-LASG, SAMIL2 (Bao et al. 2013). The atmospheric model SAMIL2, has the horizontal resolution R42 (2.81° longitude × 1.66° latitude) with 26 vertical layers in a σ–p hybrid coordinate, extending from the surface to 2.19 hPa. The mass flux cumulus parameterization of Tiedtke (1989) is used to calculate convective precipitation. The cloud scheme is a diagnostic method parameterized by low-layer static stability and relative humidity (Slingo 1980). A nonlocal scheme is employed to calculate the eddy-diffusivity profile and turbulent velocity scale, and the model incorporates nonlocal transport effects for heat and moisture (Holtslag and Boville 1993). The radiation scheme employed is an updated Edwards–Slingo scheme (Edwards and Slingo 1996; Sun and Rikus 1999). SAMIL2 is a spectral model which has been frequently used to study Asian monsoon dynamics (Duan et al. 2008; Wu et al. 2012b, He et al. 2013; Hu et al. 2015) and climate changes in various aspects (Ren et al. 2009; Wu and Zhou 2013; Zhang and Zhou 2014; Song and Zhou 2013).

The reanalysis dataset used in this study is from the ECMWF ERA-40 (Uppala et al. 2005) monthly mean data from 1979 to 1998 at http://apps.ecmwf.int/datasets/, and the precipitation dataset used is Global Precipitation Climatology Project (GPCP) (Adler et al. 2003) monthly mean data from the same period at http://www.esrl.noaa.gov/psd/data/gridded/data.gpcp.html.

2.2 Experimental design

There are two groups (HIM and HIM_NS) of experiments that have been carried out, and each group contains six experiments as shown in Table 1 with a forward slash separated. In the first group (referred to HIM00–HIM100), we firstly set the topography in HIM100 the same as Boos and Kuang (2010) that the topography between 75° E and 100° E was specified by setting surface elevations at each longitude to zero north of the point at which elevations reached two thirds of their maximum at that particular longitude (Fig. 1f). A no-mountain run (HIM00) is carried out on the basis of topography in HIM100 but the topography over the Himalaya–Iranian Plateau was set to 500 m (Fig. 1a). The topography settings in the rest of the

Table 1 Experimental design

Experiments	Topography altitude	Sensible heating
HIM00/HIM00_NS	T_0	Yes/no
HIM20/HIM20_NS	$T_0 + 0.2 \times (T_{100} - T_0)$	Yes/no
HIM40/HIM40_NS	$T_0 + 0.4 \times (T_{100} - T_0)$	Yes/no
HIM60/HIM60_NS	$T_0 + 0.6 \times (T_{100} - T_0)$	Yes/no
HIM80/HIM80_NS	$T_0 + 0.8 \times (T_{100} - T_0)$	Yes/no
HIM100/HIM100_NS	T_{100}	Yes/no

The topography in HIM100/HIM100_NS was derived the same as that in Boos and Kuang (2010) that the topography between 75° E and 100° E was specified by setting surface elevations at each longitude to zero north of the point at which elevations reached two thirds of their maximum at that particular longitude. This topography altitude was referred to T_{100} (Fig. 1f). Additionally, based on this setting, the topography where above 500 m over the regions of the Himalaya and Iranian Plateau was set to 500 m in HIM00/HIM00_NS which was referred to T_0 (Fig .1a). The topography setting in other experiments follows the formula shown in the table. The no sensible heating setting indicates that the surface is not allowed to heat the atmosphere over 20–40° N, 60–110° E where the elevation is above 500 m in each experiment, i.e., the vertical diffusive heating term in the atmospheric thermodynamic equation was set to 0

four experiments follow their expressions in Table. 1, and the topographies are shown in Fig. 1b–e.

The other group (referred to HIM00_NS–HIM100_NS) also contains six experiments in which the topography is the same as the first group (Table. 1), but the surface is not allowed to heat the atmosphere over 20–40° N, 60–110° E where the elevation is above 500 m in each experiment, i.e., the vertical diffusive heating term in the atmospheric thermodynamic equation was set to 0 in the regions of the Himalaya. All of the experiments are integrated with prescribed, seasonally varying climatological (1990–1999) sea surface temperature (SST) and sea ice. The experiments are integrated for 7 model years, in which the first 2 years are spin up time and the mean of the last 5 years are used for analysis. The differences between HIM and HIM_NS group experiments in the condition of progressive Himalaya uplift indicate the sensitivity of SASM to the topographical elevated heating.

3 Results

3.1 Model and experimental design validations

Before analyzing the sensitivity experiments, the model skills on capturing the climatological Asian summer monsoon and the sensible heating fluxes are necessary to be evaluated first. We analyzed the results from the standard Atmospheric Model Intercomparison Project (AMIP) run (Gates 1992) of SAMIL2 which was carried out with the realistic topography and observed SST and sea ice during 1979–1998 in Fig. 2 and compared with ERA40 reanalysis. Figure 2a, c, e shows the basic performances of SAMIL2 on capturing the major Asian summer climate system in the lower and upper troposphere. Although the model overestimates the precipitation magnitude in the South Asian Ocean, it captures the main features of the Asian summer monsoon pattern (Fig. 2a), performing reasonably in simulating the maximum centers over the East Arabia Sea, Bay of Bengal (BOB), and south slope of TP. It also captures the extension of East Asian summer monsoon rainbelt to North China compared to GPCP (Fig. 2b). From the low-level monsoon winds, the

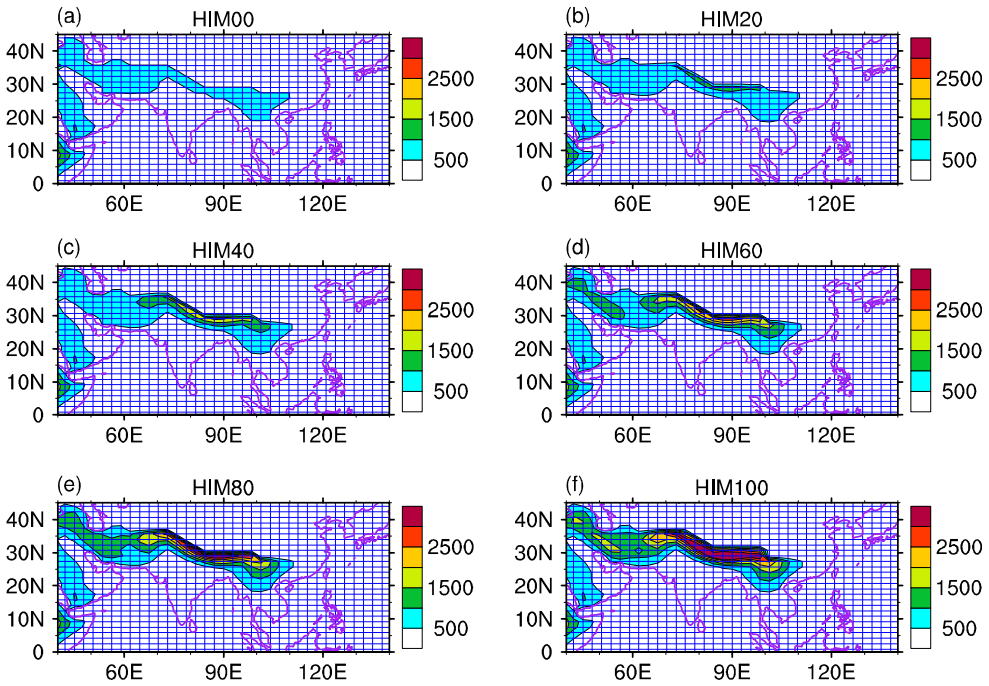

Fig. 1 Topography (m) used in the experiments of groups HIM and HIM_NS: **a** HIM00 and HIM00_NS, **b** HIM20 and HIM20_NS, **c** HIM40 and HIM40_NS, **d** HIM60 and HIM60_NS, **e** HIM80 HIM80_NS, **f** HIM100 and HIM100_NS. The actual model grid points are depicted as the *blue cross points*

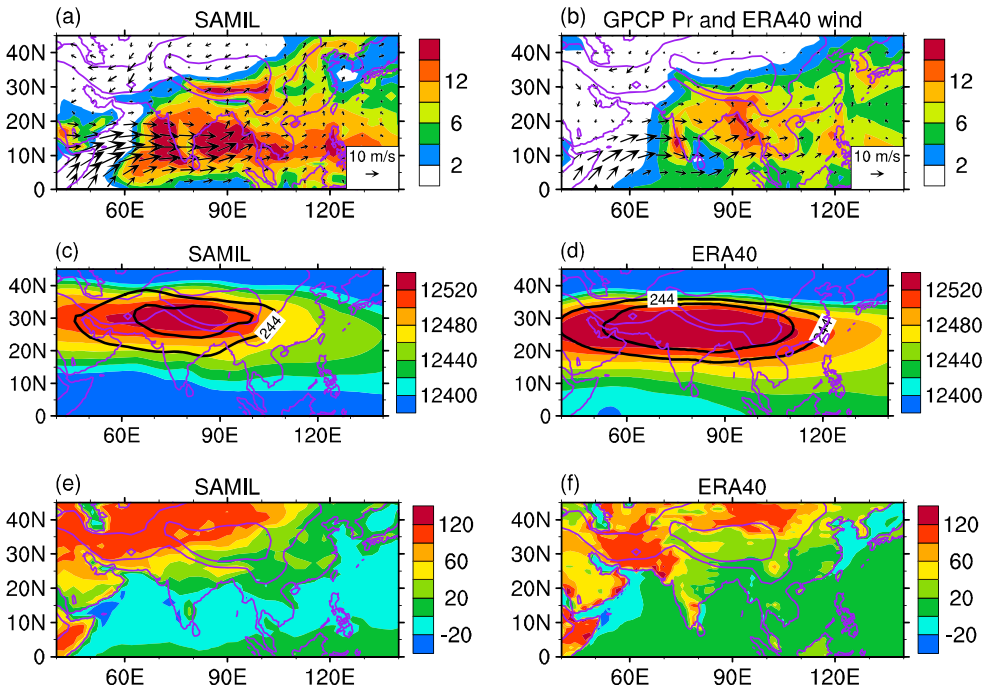

Fig. 2 Basic performances of SAMIL2 (a standard AMIP run) in simulating **a** June–July–August (JJA) mean precipitation (mm day^{-1}) and 850 hPa wind (m s^{-1}), **c** 200 hPa geopotential height (shaded, gpm) and 200–400 hPa mass-weighted mean air temperature (*black contour* for 244 K and 245 K), and **e** JJA surface sensible heating fluxes (W m^{-2}). **b** Observed 1979–1998 JJA mean precipitation (mm day^{-1}) from GPCP and 850 hPa wind (m s^{-1}) from ERA40. **d** ERA40 1979–1998 JJA mean 200 hPa geopotential height (*shaded*, gpm) and 200–400 hPa mass-weighted mean air temperature (*black contour* for 244 K and 245 K). **f** ERA40 1979–1998 JJA mean surface sensible heating fluxes (W m^{-2}). The *purple contour* indicates the topography of 1000 and 3000 m

Somali jet and the monsoon trough over BOB are well depicted compared to the ERA40 (Fig. 2b). In the upper troposphere, there exists a huge anticyclone called the South Asian High (SAH) over the Asian continent in boreal summer, characterized as the 200 hPa geopotential high center over south slope of TP (Fig. 2d) and associated with an upper troposphere temperature maximum (UTTM) in 200–400 hPa. The SAMIL2 captures the locations of the SAH and warm center quite well, except underestimates the intensity of the SAH and UTTM which is a common bias in the state-of-the-art GCMs (He and Hu 2015). At last, the simulated June–July–August (JJA) surface sensible heating fluxes are shown in Fig. 2e. The spatial pattern of simulated sensible heating is quite similar as the ERA40 (Fig. 2f), except a little overestimation on the northwest part of TP.

On the other hand, the scope of this study is to investigate the elevated heating effect of the Himalaya by isolating the Himalaya from the full topography. Therefore, whether the experimental design effectively distinguishes the heating effect on progressive uplift mountain is the key foundation. We show the model grids as the blue cross lines in Fig. 1. It can be found that there are about three to four model grids in the region where the Himalaya uplifts. From this perspective, the experimental design in this study can discern the sensible heating effect on different altitude on the slope of the Himalaya. However, because there are few grid points on the south slope of TP, these grid points can hardly stand for the drastic altitude changes of the topography which could contribute to the positive precipitation bias over the south slope of TP (Fig. 2a) in the model compared to the OBS (Fig. 2b).

3.2 Changes in precipitation and 850 hPa wind

Before analyzing the elevated heating effect of the Himalaya on Asian summer monsoon, we first show the monsoon responses in Himalaya uplift experiments (HIM00 to HIM100) and compare with the no sensible heating runs (HIM00_NS to HIM100_NS). Figure 3 shows the responses of JJA precipitation and 850 hPa wind during to the uplift of the Himalaya in the six sensitivity experiments (left column in Fig. 3) and the responses without Himalaya heating effect (right column in Fig. 3). The conspicuous features of the monsoon response are that the precipitation and 850 hPa wind are almost unchanged over Arabian Sea and Bay of Bengal (BOB), but the precipitation increases gradually over the Asian mainland when the Himalaya uplifts (Fig 3a, c, e, g, i, k). These responses are consistent with the previous studies (Kasahara et al. 1973; Liang et al. 2006; Xu et al. 2010; Wu et al. 2012b) that the basic spatial pattern of the SASM is dominantly controlled by the large-scale land–sea thermal contrast, while the strength and extension of SASM is modulated by the uplift of the highlands over the Asian continent (Abe et al. 2003; Kitoh 2004). Furthermore, the extension of the SASM in Fig. 3k has been confined to the south slope of the Himalaya, and the East Asian summer monsoon (EASM) is a little decreased from HIM00 (Fig. 3a) to HIM100 (Fig. 3k). These results are consistent with the studies of Tang et al. (2013) and Zhang et al. (2012) that the existence of the Himalaya is crucial in producing strong SASM.

On the other hand, we also compare the monsoon responses within the no sensible heating runs, i.e., HIM00_NS to HIM100_NS (Fig. 2b, d, f, h, j, l). The results show that the

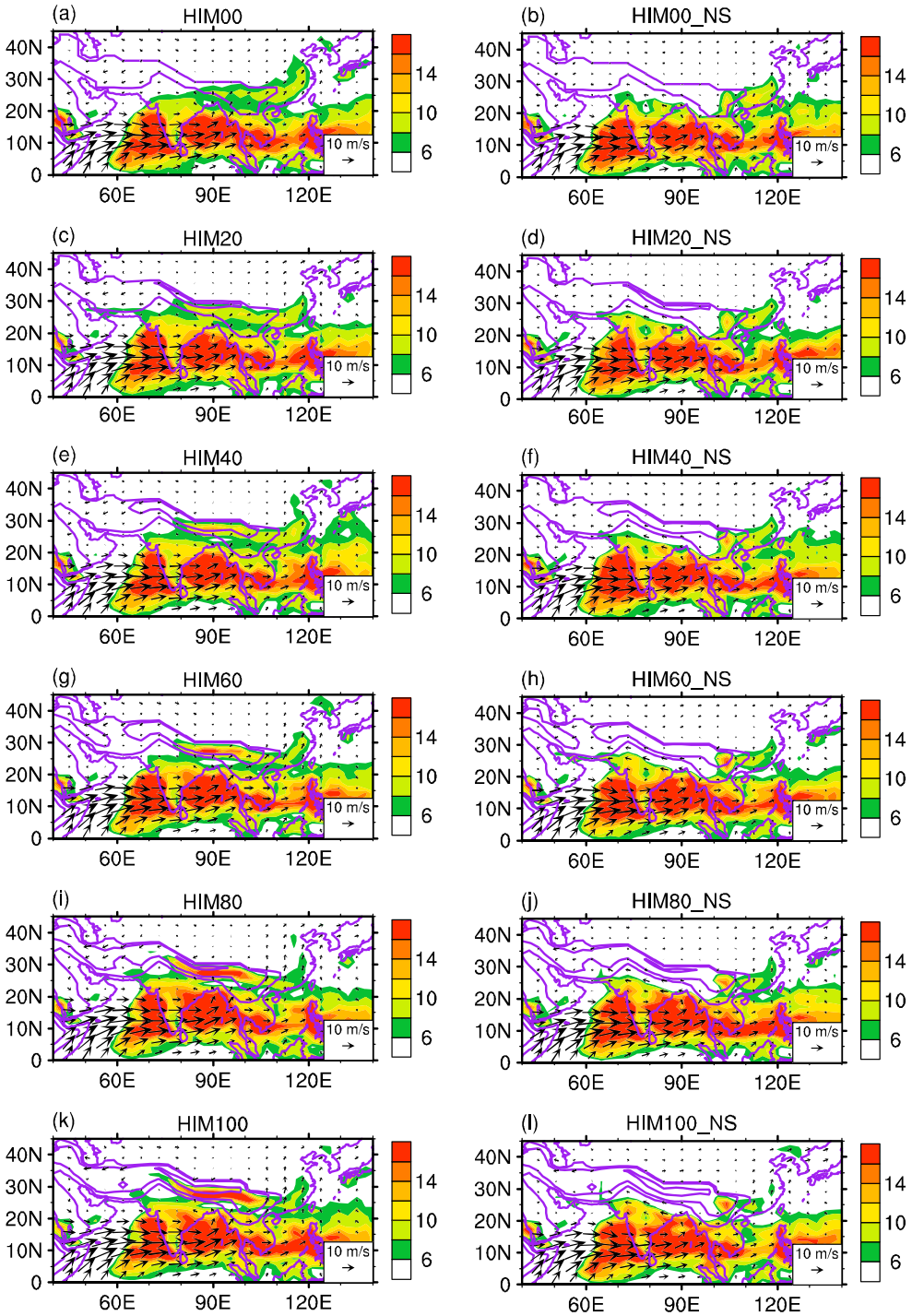

Fig. 3 June–July–August (JJA) mean precipitation (mm day^{-1}) and 850 hPa wind (m s^{-1}) simulated in **a** HIM00, **b** HIM00_NS, **c** HIM20, **d** HIM20_NS, **e** HIM40, **f** HIM40_NS, **g** HIM60, **h** HIM60_NS, **i** HIM80, **j** HIM80_NS, **k** HIM100, and **l** HIM100_NS. The *purple contour* indicates the topography of 500, 1000, and 3000 m

SASM cannot extend to the Asian inland and no significant increases in the 850 hPa wind field. These results are consistent with the theory proposed in Wu et al. (2007) that, if the south slope of the Himalaya is not heated, the air particle must move along the isentropic surface and cannot climb up on the huge mountain. Therefore, the no sensible heating experiments suggest that the blocking effect of the Himalaya is not the driven force of the strong SASM on the Asian inland.

To specifically investigate the influence of Himalaya elevated heating on SASM, we examine the differences between the HIM group (HIM00 to HIM100) and the HIM_NS group (HIM00_NS to HIM100_NS) under each the same topography setting. The differences of precipitation and 850 hPa wind between HIM00 (HIM20, HIM40, HIM60, HIM80, HIM100) and HIM00_NS (HIM20_NS, HIM40_NS, HIM60_NS, HIM80_NS, HIM100_NS) are shown in Fig. 4a–f,

respectively, which means the sensitivity of SASM to different heating altitude induced by the uplifted mountain. It is obvious that the precipitation over Asian land increases gradually and especially strengthened over the south slope of the Himalaya (Fig. 4a–f) when the Himalaya is uplifted from 500 m to almost 4000 m. Meanwhile the precipitation at tropics also decreases in the six experiments. The changes in precipitation spatial pattern are accompanied with the changes in 850 hPa wind. The 850 hPa cyclonic circulation anomalies also intensified gradually around the Himalaya from the uplift of 0 to 100 % (Fig. 4a–f) which favor the gradually intensified precipitation over the south slope of the Himalaya. Although the model overestimates the precipitation on the south slope of TP (Fig .2) which implies that the precipitation difference between HIM and HIM_NS partly involved model biases, the above results qualitatively suggest that the intensified heating effect of the Himalaya due to the uplift of mountain contributes to the strong monsoon precipitation in the South Asian inland.

3.3 Changes in the South Asian High and its thermal structure

The dominant climate system exists in upper troposphere during boreal summer is a steady semi permanent pressure system called the South Asian High (SAH) which locates above the Asian continent in the subtropics. The SAH is a huge warm anticyclone and its activities are closely linked to the variation of Asian summer monsoon (Tao and Zhu 1964; Ye and Gao 1979; Zhang et al. 2002). The responses of the SAH and its thermal structure to the elevated heating effect of the Himalaya are shown in Fig. 5. The changes in 200 hPa geopotential height (HGT) between HIM00 and HIM00_NS (Fig. 5a) shows a weak anticyclone anomaly over Asian land in correspondence to the sensible heating change in the region of the Himalaya and coincides with a positive air temperature anomaly center in the upper troposphere. When the Himalaya uplifts from 20 to 100 % (Fig. 5b–f), the HGT anomalies are gradually strengthened and expand to the west of the Himalaya, dynamically consistent with the changes in upper troposphere air temperature anomaly. The HGT anomaly shows an increase of 60 gpm when the Himalaya uplifts to the 100 % (Fig. 5f) and its main body has extended to the Iranian Plateau and Arabian Peninsula, which is almost compatible to the observed spatial scale of the SAH. These changes in SAH and its thermal structure are all induced by the sensible heating effect when the Himalaya uplifts. It is worth to note that the location and intensity of the SAH and its thermal structure in Fig. 5 is determined by the vertical gradient of heating in the free troposphere (Wu et al. 2015) which is closely related with the increase of Asian monsoon precipitation shown in Fig. 4.

Therefore, the changes in Asian summer monsoon in the two groups of Himalaya uplift experiments indicate that the elevated heating effect of the Himalaya is intensified when mountain is uplifted. It also suggests the heating effect of the Himalaya rather than its blocking effect in producing monsoon precipitation over south slope of TP, which is consistent with the conclusions in Wu et al. (2012a). Moreover, why the elevated heating effect is intensified by the uplift of the Himalaya is still not clear and needs to be further addressed. Therefore, we analyze the changes in diabatic heating and moist process in the following section to discuss the related physical processes.

4 The processes of elevated heating

4.1 The analysis in atmospheric diabatic heating

The diabatic heating act as an important forcing on the atmosphere circulations (Matsuno 1966; Webster 1972; Gill 1980). It can be sorted to four kinds: the vertical diffusion heating, the latent heating, the shortwave heating, and the longwave cooling. In general, the orders of latent heating and vertical diffusion heating are more larger than the other two radiative heatings. The vertical diffusion heating is quite shallow near the surface while the latent heating could be much stronger in the free troposphere. For convenience, we combined the shortwave heating and the longwave cooling into one radiative heating (RADH) for more straightforward physical meaning and calculated the total diabatic heating Q by adding the column integrated vertical diffusion heating (Q_{VH}), latent heating (Q_{LH}), and radiative heating (Q_{RADH}) together from the model output as shown in Eq. (1), in which P_{s} denotes the surface pressure, P_{top} denotes the pressure at the top of the model, c_{p} denotes the specific heat of air at constant pressure, and g denotes the gravitational acceleration.

$$Q = \frac{c_{\mathrm{p}}}{g}\int_{p_{\mathrm{top}}}^{p_s}(Q_{\mathrm{LH}} + Q_{\mathrm{VH}} + Q_{\mathrm{RADH}})\,dp \tag{1}$$

Figure 6 shows the difference of total diabatic heating Q between the group of HIM and HIM_NS. The responses of Q show significantly positive anomaly on the Asian mainland with the maximum center on the south slope of the Himalaya while the negative anomaly of Q appears on the tropical Indian Ocean in all of the experiments (Fig. 6a–f). The positive anomaly of Q increases gradually on the south slope of the Himalaya while the Himalaya uplifts from 0 to 100 %. The negative anomaly of Q which is located over the tropics becomes stronger when the Himalaya uplifts from 40 to 100 %; the negative centers are mainly located over the Arabian Sea and Bay of Bengal where the strong convection occurs in the SASM region. This result suggested that the

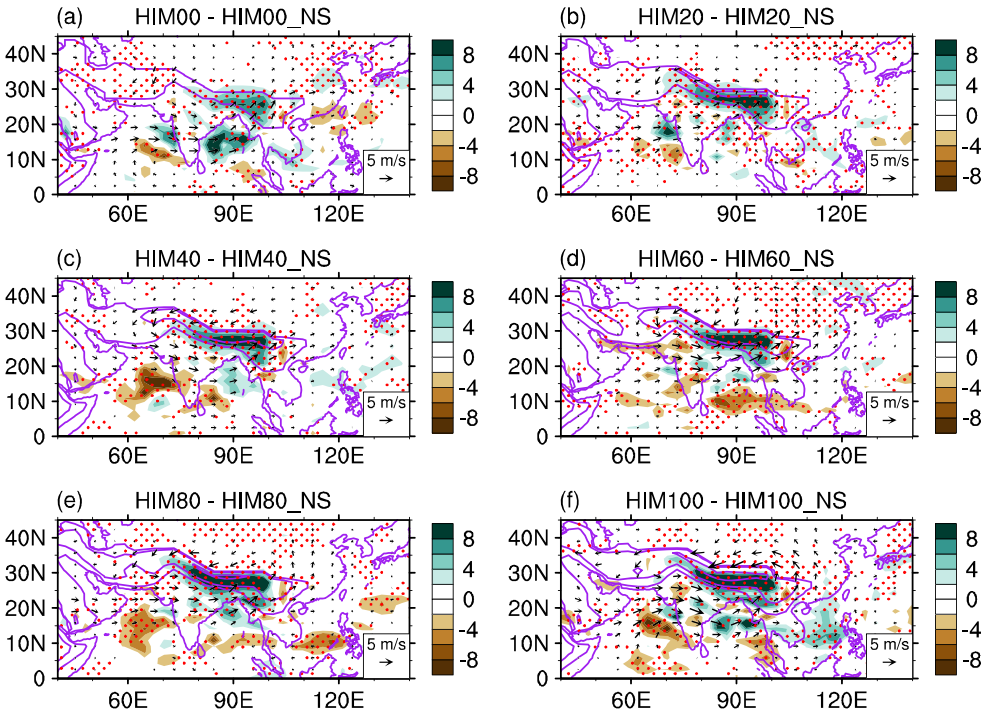

Fig. 4 Changes in JJA mean precipitation (mm day^{-1}) and 850 hPa wind (m s^{-1}) between groups HIM and HIM_NS in different mountain heights: **a** 0 %, **b** 20 %, **c** 40 %, **d** 60 %, **e** 80 %, **f** 100 %. The *red dotted areas* denote regions where the changes are statistically significant at the 95 % confidence level according to the Student's *t* test. The *purple contour* indicates the topography of 500, 1000, and 3000 m

Himalaya heating effect does not only affect the local precipitation but also has some influence on the tropical convections by triggering atmospheric circulation anomaly. The negative anomaly is also intensified according to the increased positive anomaly over the Himalaya when the mountain uplifts. Additionally, the spatial patterns of Q anomaly are very similar with the patterns of precipitation (Fig. 4) which implies that the changes in diabatic heating is dominant by changes in the latent heating.

We further investigate the sensitivity of each kind of diabatic heating over the region of 75°–100° E, 24°–32° N (Fig. 7). It is obvious that the latent heating major contributes to the total diabatic heating with a magnitude of 100–

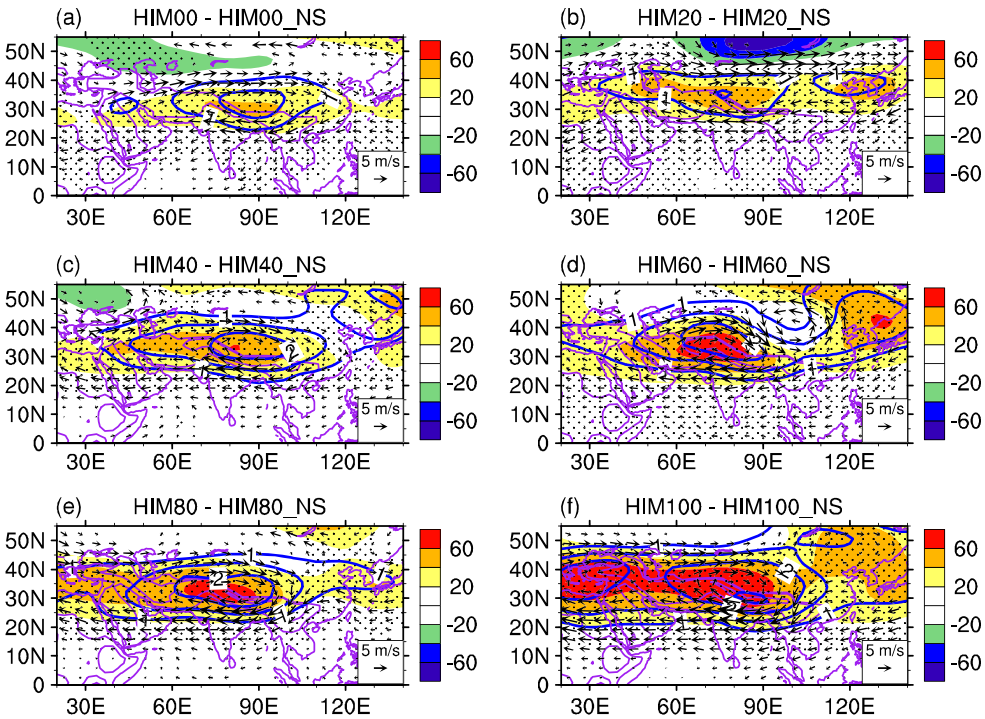

Fig. 5 Changes in JJA mean 200 hPa geopotential height (gpm, *shaded*), 200 hPa wind (m s^{-1}, vector) and 200–400 hPa mass-weighted mean air temperature (K, *blue contour*) between groups HIM and HIM_NS in different mountain heights: **a** 0 %, **b** 20 %, **c** 40 %, **d** 60 %, **e** 80 %, **f** 100 %. The *black dotted areas* denote regions where the changes of geopotential height are statistically significant at the 95 % confidence level according to the Student's *t* test. The purple contour indicates the topography of 500, 1000, and 3000 m

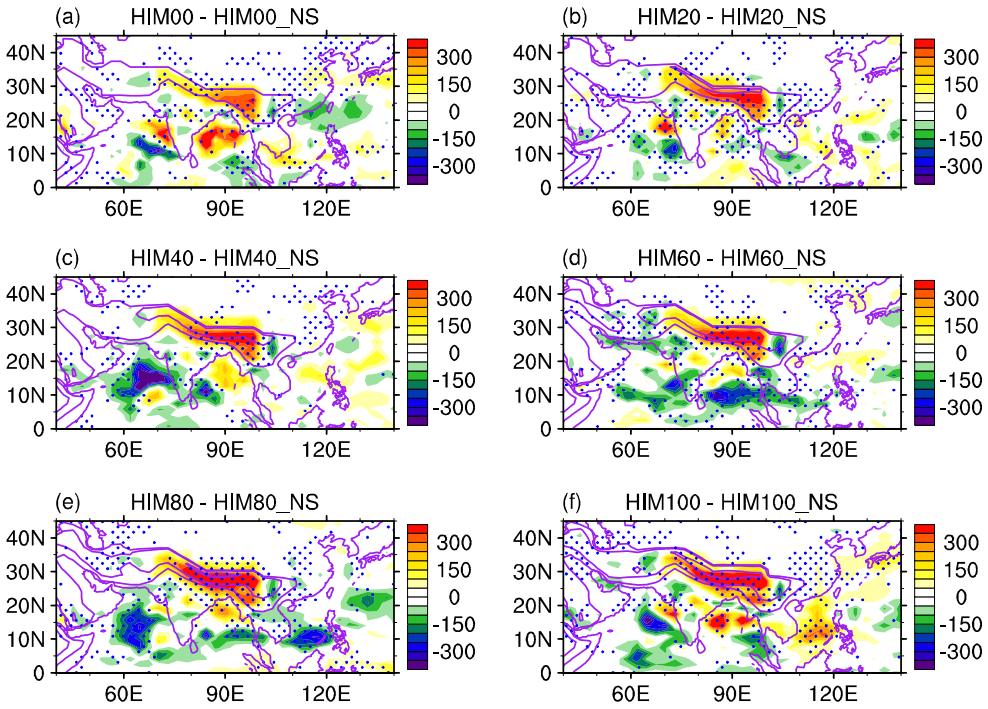

Fig. 6 Changes in JJA mean total diabatic heating (W m^{-2}) between groups HIM and HIM_NS in different mountain heights: **a** 0 %, **b** 20 %, **c** 40 %, **d** 60 %, **e** 80 %, **f** 100 %. The *blue dotted areas* denote regions where the changes are statistically significant at the 95 % confidence level according to the Student's *t* test. The *purple contour* indicates the topography of 500, 1000, and 3000 m

300 W m^{-2} while the vertical heat diffusion shows an order smaller, and the contributions of radiative heating can be neglected. Furthermore, the increases of latent heating are approximately linear when the Himalaya uplifts from 0 to 80 %, but the vertical diffusion heating is almost not changed. These results demonstrate an important fact that the strength of vertical heating diffusion does not change when the Himalaya uplifts, but it could induce stronger latent heating release in proportion to the mountain uplift scale. It implies that the condensation process on the south slope of the Himalaya is a crucial link between the elevated heating effect of the Himalaya and the changes in the SASM. Therefore, the study on the changes in moist process in the two groups of experiments is beneficial for us to understand the thermodynamics of the elevated heating and its influence to the SASM.

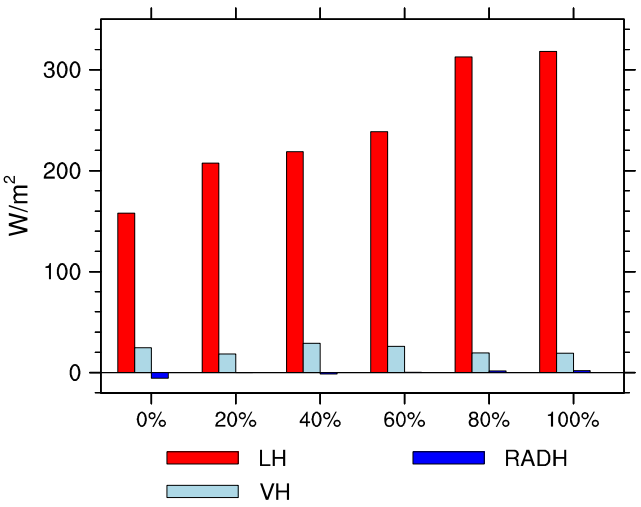

Fig. 7 Regional mean (24–32° N, 75–100° E) JJA column total latent heating (*LH*) (W m^{-2}), vertical diffusing heating (*VH*) (W m^{-2}), and radiation heating (*RADH*) (W m^{-2}) for different mountain heights in group HIM

4.2 The analysis in moist process

For the climate mean state we discussed here, the changes in the column water vapor, the surface evaporation, and the precipitation are the most three important terms in the hydrological cycle. The responses of the precipitation due to the elevated heating effect of the Himalaya are already shown in Fig. 4. Thus, we show the responses of atmospheric water vapor and surface evaporation in the following paragraph to have a complete image on the moist process over the South Asia when Himalaya uplifts.

Figure 8 shows the responses of water vapor path to the elevated heating effect of the Himalaya in each uplift level (HIM group minus HIM_NS group). It is evident that the positive water vapor path anomaly covers the region of the Himalaya and north Indian flatland in all of the cases. Quantitative calculations of the water vapor path over the region 75°–100° E, 24°–32° N show 6.6 kg m^{-2} (Fig. 8a), 5.0 kg m^{-2} (Fig. 8b), 4.9 kg m^{-2} (Fig. 8c), 4.3 kg m^{-2} (Fig. 8d), 6.1 kg m^{-2} (Fig. 8e), and 4.6 kg m^{-2} (Fig. 8f) in respective to the Himalaya uplifted by 0, 20, 40, 60, 80, and 100 %. However, the spatial pattern of the increased water vapor path shows remarkable differences between the south slope of the Himalaya and north Indian flatland in each uplift case. When the Himalaya is not uplifted (Fig. 8a), the major

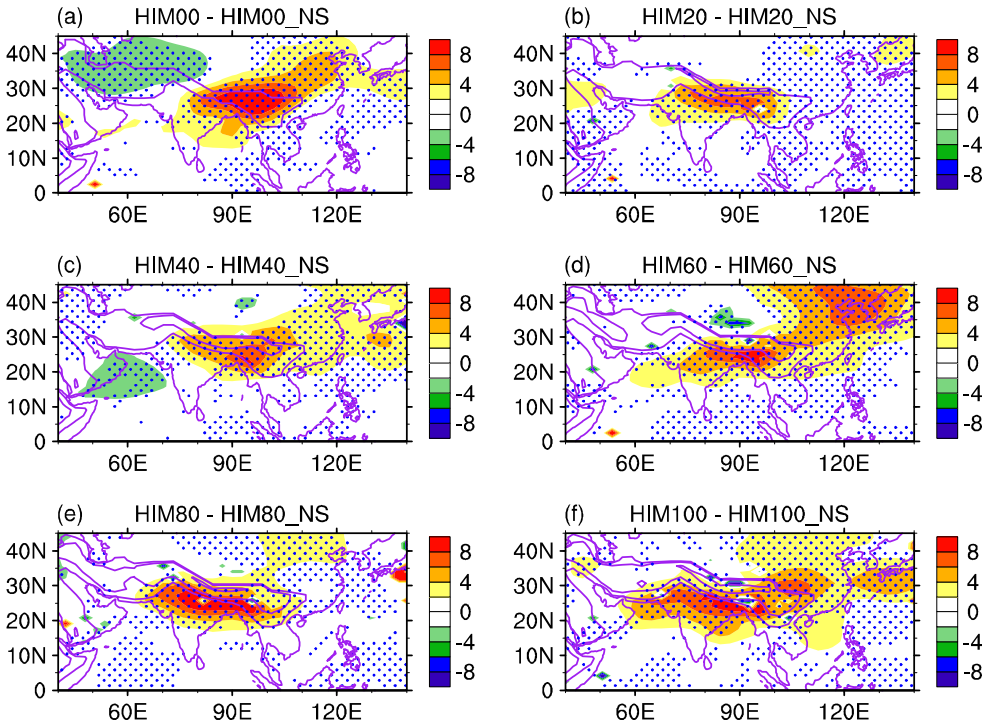

Fig. 8 Changes in JJA mean water vapor path (kg m^{-2}) between groups HIM and HIM_NS in different mountain heights: **a** 0 %, **b** 20 %, **c** 40 %, **d** 60 %, **e** 80 %, **f** 100 %. The *blue dotted areas* denote regions where the changes are statistically significant at the 95 % confidence level according to the Student's *t* test. The *purple contour* indicates the topography of 500, 1000, and 3000 m

part of the increased water vapor path locates over Himalaya where the sensible heating is suppressed. However, when the Himalaya uplifts from 20 to 100 % (Fig. 8b–f) the responses of water vapor path due to elevated heating increase over the north Indian flatland while reduce over the south slope of the Himalaya.

The responses of the surface evaporation due to the elevated heating of the Himalaya are shown in Fig. 9. The spatial pattern of the evaporation shows an overall increase over the south slope of the Himalaya with the same region of the sensible heating change. There are almost no obvious differences within the evaporation changes (Fig. 9a–f) when the Himalaya is uplifted. Quantitative calculations of the changes in evaporation over the region 75°–100° E, 24°–32° N show 1.5, 1.6, 1.6, 1.7, 1.9, and 1.7 mm day^{-1} in respective to the Himalaya uplifted by 0, 20, 40, 60, 80, and 100 %. However, the maximum of the evaporation is about 2 mm day^{-1} in all the cases and is comparable to the magnitude of precipitation changes in the uplift of 0 % (Fig. 4a) and 20 % (Fig. 4b) but far less than the precipitation when the Himalaya uplifts to 100 % (Fig. 4f). This result indicates that local feedback between evaporation and precipitation in a flat case is not enough to produce strong SASM. It also reveals that the positive feedback between the precipitation and low troposphere water vapor convergence on the south slope of the Himalaya is the primary cause of the strong SASM. The responses of the atmospheric water vapor (Fig. 8), surface evaporation (Fig. 9), and precipitation (Fig. 4) over the South Asian land suggest that the moist condensations are gradually intensified but the vertical diffusion heating is almost not changed (Fig. 7) in the uplift cases from HIM00 to HIM100. Thus, The condensation process appears to be the key findings that cause the strong heating effect over the south slope of the Himalaya.

From the perspective of the moist convective adjustment, the air parcel is firstly lifted up by external forcing from the ground to the lifted condensation level (LCL) and follows the moist adiabats thereafter. The external forcing here usually denotes the sensible heating at surface. For the air particles over the south slope of the Himalaya, they are easily to be lifted to the LCL because of the sensible heating on the south slope of the Himalaya directly heating the air in the lower troposphere. This process is investigated by the following figures. We calculated the LCL in the six experiments of group HIM in Fig. 10 separately. The LCL in the HIM00 case (Fig. 10a) is about 3000 m. Because the vertical diffusion heat decreases rapidly to 0 from the ground to approximately 3000 m in the low troposphere (Wu et al. 2008), the air parcel is hard to be lifted up by the external forcing such as the local heat flux in the case of HIM00. However, when the Himalaya uplifts from 20 to 100 %, the LCL reduced gradually over the south slope of the Himalaya (Fig. 10b–f). While the Himalaya has uplifted to 100 %, the LCL is less than 1000 m over the south slope of the Himalaya, which indicates that the air

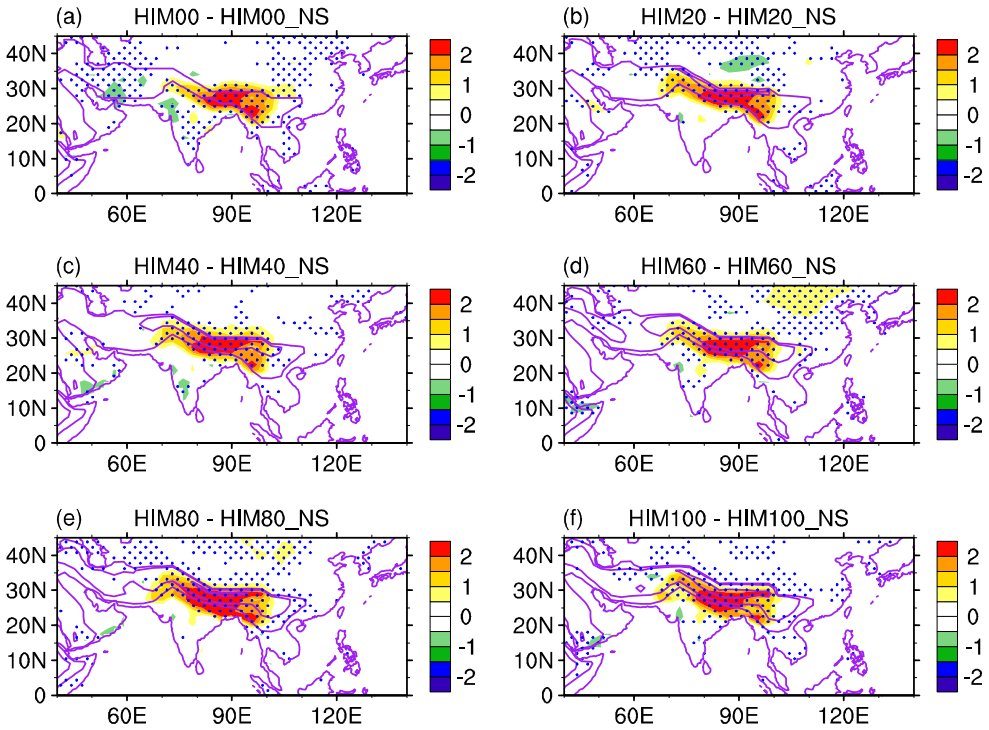

Fig. 9 Changes in JJA mean evaporation (mm day^{-1}) between groups HIM and HIM_NS in different mountain heights: **a** 0 %, **b** 20 %, **c** 40 %, **d** 60 %, **e** 80 %, **f** 100 %. The *blue dotted areas* denote regions where the changes are statistically significant at the 95 % confidence level according to the Student's *t* test. The *purple contour* indicates the topography of 500, 1000, and 3000 m

parcel is much more easer to be lifted to the condensation level. Consequently, the condensation moisturing (the mass of the water vapor condensed from gas phase to liquid phase) between groups HIM and HIM_NS is well coordinated with the changes in LCL as shown in Fig. 11. The condensation moisturing is quite weak when the Himalaya remains flat (Fig. 11a), but increases gradually over the south slope of the Himalaya when the mountain is uplifted (Fig. 11b–f). The analysis of the moist process over the South Asian land indicates that the sensible heating on the Himalaya surface is more efficient in lifting the air parcel to the condensation level than its direct heating effect on producing SASM. The moist convection is easier to occur and

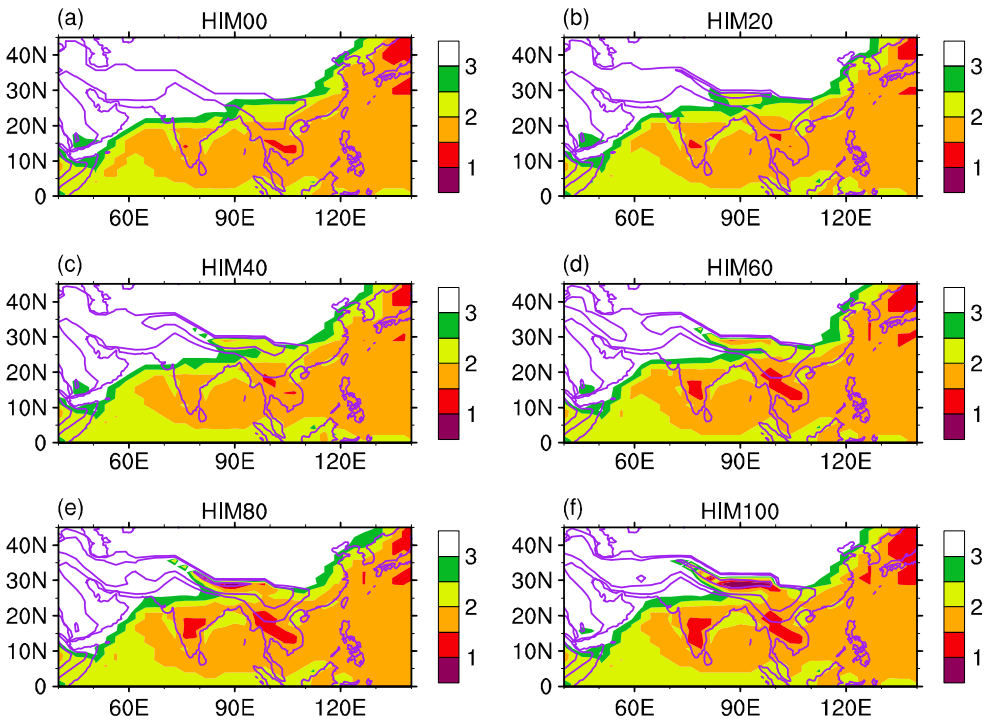

Fig. 10 The simulated JJA mean lifted condensation level (km) in a HIM0, b HIM20, c HIM40, d HIM60, e HIM80, and f HIM100. The purple contour indicates the topography of 500, 1000, and 3000 m

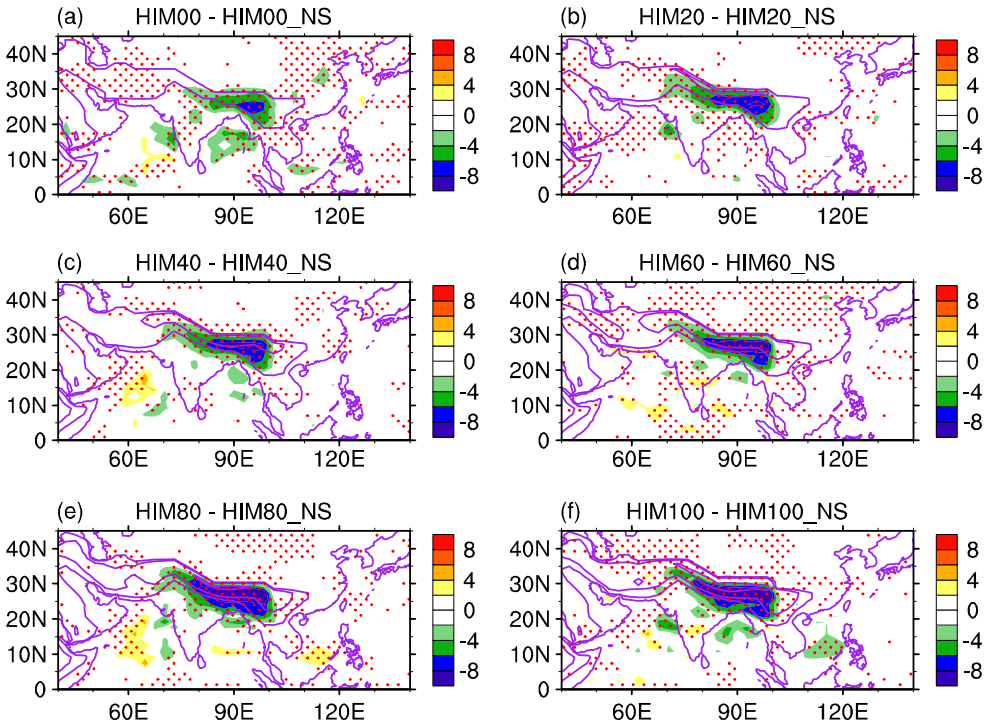

Fig. 11 Changes in JJA mean condensation moisturing (g kg^{-1} day^{-1}) between groups HIM and HIM_NS in different mountain heights: **a** 0 %, **b** 20 %, **c** 40 %, **d** 60 %, **e** 80 %, **f** 100 %. The *red dotted areas* denote regions where the changes are statistically significant at the 95 % confidence level according to the Student's *t* test. The *purple contour* indicates the topography of 500, 1000, and 3000 m

causes the positive feedback between the latent heating and large-scale convergence when the Himalaya uplifts to a certain height.

5 Conclusions and discussions

The influences of the elevated heating effect of the Himalaya on the South Asian summer monsoon are investigated based on a series of numerical experiments in this study. We isolate the topography of the Himalaya from the whole Tibetan Plateau in the experiments and consider its different altitudes by 0 % (HIM00), 20 % (HIM20), 40 % (HIM40), 60 % (HIM60), 80 % (HIM80), and 100 % (HIM100) in the first group (HIM). The other group of experiments (HIM_NS) have been performed by preventing the surface sensible heating to heat the atmosphere (HIM00_NS, HIM20_NS, HIM40_NS, HIM60_NS, HIM80_NS, HIM100_NS) but with the same elevations as in the first group. The differences between group HIM and HIM_NS are regarded as the responses to the elevated heating effect of the Himalaya. The major conclusions obtained from the sensitivity experiments are summarized as follows.

The results of HIM group indicate that the SASM precipitation gradually intensified over the South Asian land when the Himalaya uplifts. The simulated precipitation spatial pattern in HIM100 (100 % uplift) is similar to the observed one over the South Asian region. However, due to the missed topography of the plateau part of TP, the precipitation over Central Asia disappeared in the HIM100. Furthermore, the extension and intensity of the East Asian summer monsoon have been reduced when the Himalaya uplifts from 0 to 100 %. The evolutions of the SASM from HIM00 to HIM100 are consistent with the simulation results of Kitoh (2004) who used a coupled model to test the influences of different mountain heights on the Asian summer monsoon. The north branch of SASM is gradually established on the south slope of the Himalaya.

The differences between HIM and HIM_NS indicate that the formation of SASM over the South Asian land is quite sensitive to the elevated heating effect of the Himalaya. The monsoon precipitation on the south slope of the Himalaya and lower troposphere cyclonic circulation gradually intensified when surface sensible heating elevated as the Himalaya uplifts. Moreover, the increased latent heating in the free troposphere act as an important heating source in the formation of the SASM structure: The upper troposphere air becomes warmer and the South Asian High is strengthened and extends west over the Asian continent.

The analysis of the diabatic heating and moist process suggested that the surface sensible heating directly heats the air in the lower troposphere on its south slope, and the moist air is easier to be lifted up to the LCL when the Himalaya uplifts. Therefore, the condensation moisturing increases correspondingly and leads to the increases of precipitation and latent heating in the free troposphere. Because the latent heating strengthened mainly from 300 to 700 hPa, the vertical inhomogeneous diabatic heating force an anticyclone in the upper troposphere and moist convergence in the lower

troposphere which forms the positive feedback between the moist convection and large-scale circulations.

This study highlights the elevated heating effect of the Himalaya is crucial in triggering moist convections and modulating Asian summer monsoon over the South Asian inland. The numerical simulation results also testify the assumption raised in Ye and Gao (1979) and Wu et al. (1997) that the sensible heating of TP is so important because it directly heats the air in the middle and lower troposphere. However, currently, there are still shortages on the accurate estimation of the sensible heating fluxes over the Tibetan Plateau. For example, Ma et al. (2011) emphasized that the parameterization methodology on estimating heat fluxes over TP is not an easy issue, and more field observations, more accurate radiation transfer models, and more satellites data have to be used to reduce the uncertainty in the calculation of heat fluxes over TP. Yang et al. (2009) developed a new scheme on estimating the heat fluxes over TP based on the statistical relationships derived from high-resolution experimental data and found it is much better than previous schemes. Chen et al. (2013) developed a DEM (digital elevation model)-based radiation model to estimate instantaneous clear sky solar radiation for obtaining accurate energy absorbed by the mountain surface. Therefore, the new schemes and datasets should be used in parameterizing the heat fluxes over TP in the GCMs to get more realistic simulation on the TP climatic effect studies.

Another challenge in studying TP dynamics is the development of the high-resolution global models. The Himalaya is very steep in the reality and its influence to Asian climate calls for a finer model with 10–25 km resolution to distinguish the mountain with the whole TP. Bacmeister et al. (2014) compared the simulation results between the high-resolution (0.23° latitude × 0.31° longitude) model, Community Atmosphere Model versions 5 and 4 (CAM5 and CAM4), and a typical resolution of 0.9° latitude × 1.25° longitude. Overall, the simulated climate of the high-resolution experiments is not dramatically better than that of their low-resolution counterparts, but improvements appear primarily where topographic effects may be playing important role, such as the summertime Indian monsoon. Furthermore, to improve the simulation ability of high-resolution model, the improvements in the model physics and introduction of nonhydrostatic framework are both necessary (Pope et al. 2007; Satoh 2008).

Additionally, air–sea interaction need to be considered in the climate simulation of the TP elevated heating impactions. Many studies (Kitoh 1997; Okajima and Xie 2007; Koseki et al. 2008) claimed that the role of air–sea interaction is very important to the orgraphic effects on the monsoons and global climate change. Kitoh (1997) shows that the global mean sea surface temperature (SST) dropped 1.4 °C with the mountain uplift, mainly due to increased lower tropospheric clouds in the subtropical eastern Pacific. Okajima and Xie (2007) indicates that the response is opposite between the atmospheric and coupled models during spring and early summer when the global orography is removed, while the SST cooling is responsible for all these differences. Therefore, the responses of SASM and global climate to the elevated heating effect of TP could be very different when considering the air–sea coupling. Further numerical experiments and analysis are suggested to be carried out to get a more comprehensive understanding on the roles of the TP on climate change.

Acknowledgments This study was jointly funded by the China Meteorological Administration (No. GYHY201406001), the National Key Basic Research Program of China (Grant 2014CB953904), the National Natural Science Foundation of China (Grants 41405091, 91337110), the State Key Laboratory of Loess and Quaternary Geology (Grant SKLLQG1216), and Strategic Leading Science Projects of the Chinese Academy of Sciences (Grant XDA11010402).

References

Abe M, Kitoh A, Yasunari T (2003) An evolution of the Asian summer monsoon associated with mountain uplift simulation with the MRI atmosphere-ocean coupled GCM. J Meteorol Soc Japan 81(5):909–933

Adler RF et al. (2003) The Version-2 Global Precipitation Climatology Project (GPCP) monthly precipitation analysis (1979–present). J Hydrometeor 4:1147–1167

Bacmeister JT et al. (2014) Exploratory high-resolution climate simulations using the Community Atmosphere Model (CAM). J Clim 27: 3073–3099

Bao Q et al. (2013) The Flexible Global Ocean-Atmosphere-Land System Model, Spectral Version 2: FGOALS-s2. Adv Atmos Sci 30:561–576

Boos WR, Kuang ZM (2010) Dominant control of the South Asian monsoon by orographic insulation versus plateau heating. Nature 463: 218–222

Boos WR, Kuang ZM (2013) Sensitivity of the South Asian monsoon to elevated and non-elevated heating. Sci Rep 3:1192. doi:10.1038/srep01192

Chen LX, Liu JP, Zhou XJ, Wang PX (1999) Impact of uplift of Qinghai-Xizang Plateau and change of land-ocean distribution on climate over Asia. Quat Sci 4:314–329

Chen X, Su Z, Ma Y, Yang K, Wang B (2013) Estimation of surface energy fluxes under complex terrain of Mt. Qomolangma over the Tibetan Plateau. Hydrol Earth Syst Sci 17:1607–1618

Duan AM, Wu GX (2005) Role of the Tibetan Plateau thermal forcing in the summer climate patterns over subtropical Asia. Clim Dyn 24: 793–807. doi:10.1007/s00382-004-0488-8

Duan AM, Wu GX, Liang XY (2008) Influence of the Tibetan Plateau on the summer climate patterns over Asia in the IAP/LASG SAMIL model. Adv Atmos Sci 25(4):518–528

Edwards JM, Slingo A (1996) A studies with a flexible new radiation code. I: choosing a configuration for a large-scale model. Quart J Roy Meteor Soc 122:689–720

Gates WL (1992) AMIP: the Atmospheric Model Intercomparison Project. Bull Amer Meteor Soc 73(12):1962–1970

Gill AE (1980) Some simple solutions for heat-induced tropical circulation. Quart J Roy Meteor Soc 106:447–462

Hahn DG, Manabe S (1975) The role of mountains in the South Asian monsoon circulation. J Atmos Sci 32:1515–1541

He B et al. (2013) Influences of external forcing changes on the summer cooling trend over East Asia. Clim Chang 117(4):829–841

He B, Hu WT (2015) Assessment of the summer South Asian high in eighteen CMIP5 models. Atmos Oceanic Sci Lett 8:33–38

Holtslag AAM, Boville BA (1993) Local versus nonlocal boundary-layer diffusion in a global climate model. J Clim 6:1825–1842

Hu WT, Duan AM, Wu GX (2015) Impact of subdaily air–sea interaction on simulating intraseasonal oscillations over the tropical Asian monsoon region. J Clim 28:1057–1073

Jiang DB, Ding ZL, Drange H, Gao YQ (2008) Sensitivity of East Asian climate to the progressive uplift and expansion of the Tibetan Plateau under the Mid-Pliocene boundary conditions. Adv Atmos Sci 25(5):709–722

Kasahara A, Sasmori T, Washington WM (1973) Simulation experiments with a 12-layer stratospheric global circulation model. I: dynamical effect of the earth's orography and thermal influence of continentality. J Atmos Sci 30:1229–1251

Kitoh A (1997) Mountain uplift and surface temperature changes. Geophy Res Let 24(2):185–188

Kitoh A (2004) Effects of mountain uplift on East Asian summer climate investigated by a coupled atmosphere-ocean GCM. J Clim 17(4): 783–802

Kitoh A, Motoi T, Arakawa Q (2010) Climate modeling study on mountain uplift and Asian monsoon evolution. Geological Society, Special Publications 342:293–301

Koseki S, Watanabe M, Kimoto M (2008) Role of the midlatitude air-sea interaction in orographically forced climate. J Meteor Soc Japan 86(2):335–351

Liang XY, Liu YM, Wu GX (2006) Roles of tropical and subtropical land-sea distribution and the Qinghai-Xizang Plateau in the formation of the Asian summer monsoon. Chin J Geophys 49(4):983–992(in Chinese)

Liu XD (1999) Influences of Qinghai-Xizang (Tibet) Plateau uplift on the atmospheric circulation, global climate and environment changes. Plateau Meteorology 18(3):321–332(in Chinese)

Liu XD, Yin ZY (2002) Sensitivity of East Asian monsoon climate to the uplift of the Tibetan Plateau. Palaeogeogr Palaeoclimatol Palaeoecol 183:223–245

Liu YM et al. (2012) Revisiting Asian monsoon formation and change associated with Tibetan Plateau forcing: II. Change. Clim Dyn 39: 1183–1195

Ma YM, Wang YJ, Zhong L, Wu RS, Wang SZ (2011) The characteristics of atmospheric turbulence and radiation energy transfer and the structure of atmospheric boundary layer over the northern slope area of Himalaya. J Meteor Soc Japan 89:345–353

Manabe S, Terpstra TB (1974) The effects of mountains on the general circulation of the atmosphere as identified by numerical experiments. J Atmos Sci 31(1):3–42

Matsuno T (1966) Quasi-geostrophic motions in the equatorial area. J Meteor Soc Japan Ser II 44:25–43

Okajima H, Xie SP (2007) Orgraphic effects on the northwestern Pacific monsoon: role of air-sea interaction. Geophy Res Lett 34:L21708

Pope V et al. (2007) The Met Office Hadley Centre climate modelling capability: the competing requirements for improved resolution, complexity and dealing with uncertainty. Phil Trans R Soc A 365: 2635–2657

Ren RC, Wu GX, Cai M, Yu JJ (2009) Winter season stratospheric circulation in the SAMIL/LASG general circulation model. Adv Atmos Sci 26(3):451–464

Satoh M (2008) Nonhydrostatic icosahedral atmospheric model (NICAM) for global cloud resolving simulations. J Comput Phys 227:3486–2514

Slingo JM (1980) A cloud parameterization scheme derived from GATE data for use with a numerical model. Quart J Royal Meteor Soc 106: 747–770

Song FF, Zhou TJ (2013) FGOALS-s2 simulation of upper-level jet streams over East Asia: mean state bias and synoptic-scale transient eddy activity. Adv Atmos Sci 30(3):739–753. doi:10.1007/s00376-012-2212-7

Sun ZA, Rikus (1999) Parameterization of effective radius of cirrus clouds and its verification against observations. Quart J Royal Meteor Soc 125:3037–3056

Tang H, Micheels A, Eronen JT, Ahrens B, Fortelius M (2013) Asynchronous responses of East Asian and Indian summer monsoons to mountain uplift shown by regional climate modeling experiments. Clim Dyn 40:1531–1549

Tao SY, Zhu FK (1964) The variation of 100 mb circulation over South Asia in summer and its association with March and withdraw of West Pacific Subtropical High. Acta Meteor Sin 34:385–395

Tiedtke M (1989) A comprehensive mass flux scheme for cumulus parameterization in large-scale models. Mon Wea Rev 117:1779–1800

Uppala SM et al. (2005) The ERA-40 re-analysis. Quart J R Meteorol Soc 131:2961–3012

Webster PJ (1972) Response of the tropical atmosphere to local, steady forcing. Mon Wea Rev 100:518–541

Wu B, Zhou TJ (2013) Relationships between East Asian-western North Pacific monsoon and ENSO simulated by FGOALS-s2. Adv Atmos Sci 30(3):713–725. doi:10.1007/s00376-013-2103-6

Wu GX, He B, Liu YM, Bao Q, Ren CC (2015) Location and variation of the summertime uppertroposphere temperature maximum over South Asia. Clim Dyn 45(9-10):2757–2774

Wu GX, Liu YM, Yu JJ, Zhu XY, Ren RC (2008) Modulation of land–sea distribution on air–sea interaction and formation of subtropical anticyclones. Chinese J Atmos Sci 32(4):720–740(in Chinese)

Wu GX et al (1997) Sensible heat driven air-pump over the Tibetan Plateau and its impacts on the Asian summer monsoon. Collections on the Memory of Zhao jiuzhang, eds Ye DZ, et al. Chinese Science Press, Beijing

Wu GX et al. (2007) The influence of mechanical and thermal forcing by the Tibetan Plateau on Asian climate. J Hydrometeorol 8:770–789

Wu GX, Zhang YS (1998) Tibetan Plateau forcing and the timing of the monsoon onset over South Asia and the South China Sea. Mon Wea Rev 126:913–927

Wu GX et al. (2012a) Thermal control on the Asian summer monsoon. Sci Rep 2:404. doi:10.1038/srep00404

Wu GX et al. (2012b) Revisiting Asian monsoon formation and change associated with Tibetan Plateau forcing: I. Formation. Clim Dyn 39: 1169–1181

Xu ZF, Qian YF, Fu CB (2010) The role of land-sea distribution and orography in the Asian monsoon. Part II: orography. Adv Atmos Sci 27(3):528–542

Yang K, Qin J, Guo XF, Zhou DG, Ma YM (2009) Method development for estimating sensible heat flux over the Tibetan Plateau from CMA data. J Appl Meteorol Clim 48:2474–2486

Ye DZ, Gao YX (1979) Meteorology of the Qinghai-Xizang Plateau. Chinese Science Press, Beijing 278 pp (in Chinese)

Zhang LX, Zhou TJ (2014) An assessment of improvements in global monsoon precipitation simulation in FGOALS-s2? Adv Atmos Sci 31(1):165–178

Zhang Q, Wu GX, Qian YF (2002) The bimodality of the 100 hPa South Asia High and its relationship to the climate anomaly over East Asia in summer. J Meteor Soc Japan 80(4):733–744

Zhang R, Jiang DB, Liu XD, Tian ZP (2012) Modeling the climate effects of different subregional uplifts within the Himalaya-Tibetan Plateau on Asian summer monsoon evolution. Chin Sci Bull 57:4617–4626